Supporting information

Gold Nanorod-Melanin Hybrids for Enhanced and Prolonged Photoacoustic Imaging in the Near-Infrared-II Window

Wonjun Yim[1]†, Jiajing Zhou[2]†, Yash Mantri[3], Matthew N. Creyer[2], Colman A. Moore[2], and Jesse V. Jokerst[1,3,4,*]

[1]Materials Science and Engineering Program

[2]Department of Nanoengineering

[3]Department of Bioengineering

[4]Department of Radiology

University of California San Diego, 9500 Gilman Dr., La Jolla, CA 92093, United States

* Correspondence and requests for materials should be addressed to jjokerst@ucsd.edu

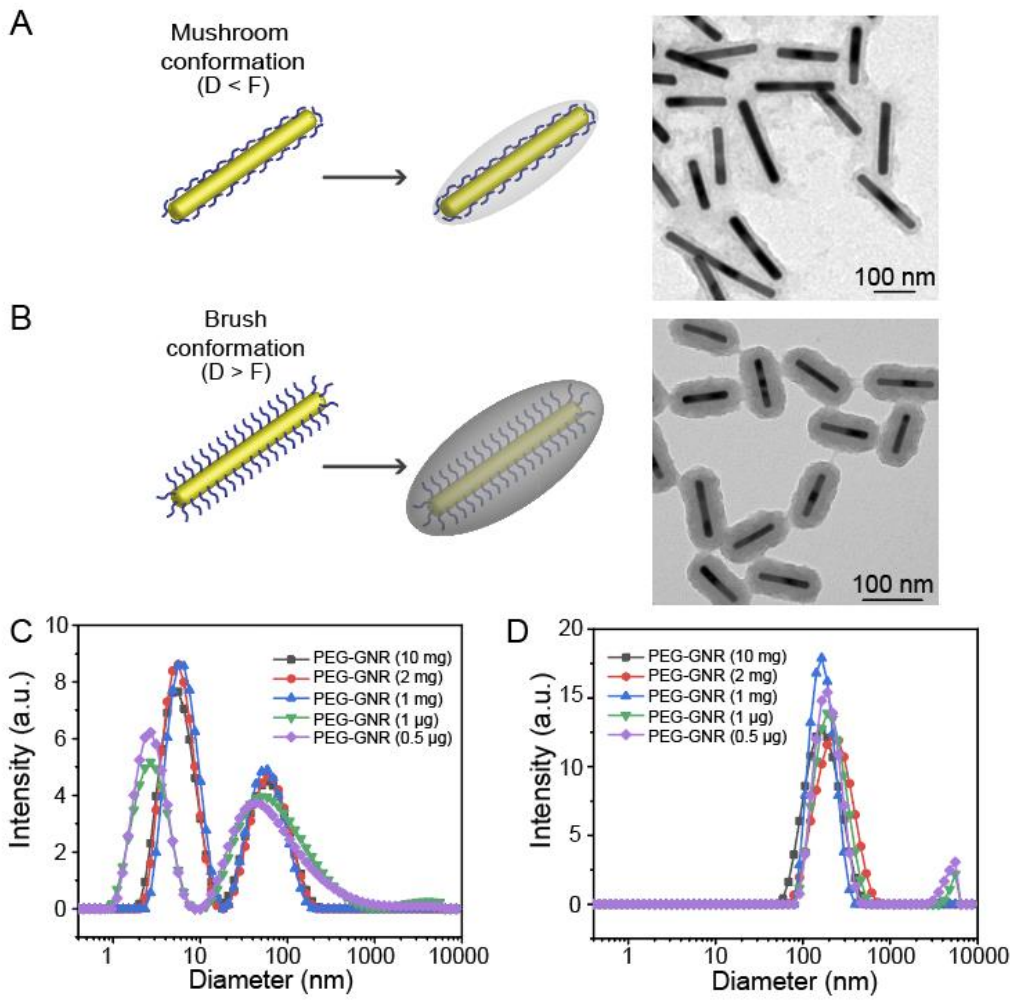

Figure S1. Mushroom and brush conformation. PEG chains can form either mushroom or brush conformations. (A) PEG chains formed the mushroom conformation and PDA coating was instable when we used a small amount of PEG-SH. (B) PEG chains made the brush conformation when we used large amount of PEG-SH (>1 mg). PDA coating became stable and uniform, showing colloidal stability. (C) DLS data of PEGylated GNRs at different concentration of PEG-SH: 10 mg, 2 mg, 1 mg, 1 μg, and 0.5 μg. (D) DLS data of PDA coated GNRs replaced by different amounts of PEG chain. GNRs were aggregated, and PDA coating was unstable when we used 1 μg, and 0.5 μg (mushroom conformation). The mass concentration of GNR was 200 μg/mL, and we used 1:1 ratio of GNR to dopamine concentration (4 mg/mL).

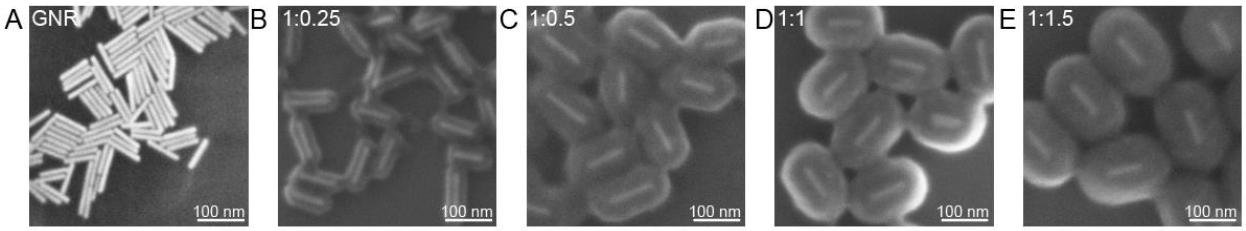

Figure S2. SEM images of GNR@PDAs. (A) GNR, (B) GNR@PDA15, (C) GNR@PDA25, (D) GNR@PDA50, and (E) GNR@PDA70.

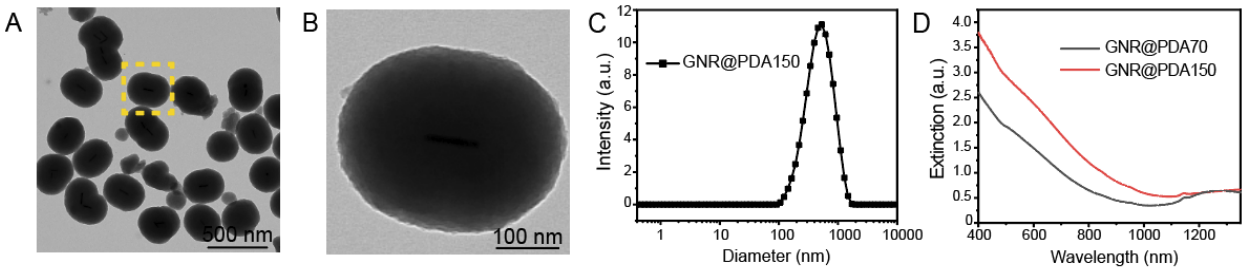

Figure S3. (A) GNRs aggregated when we used an excess of dopamine. (B) The yellow dotted square shows TEM image of a single GNR@PDA particle with PDA thickness of 150 nm (referred as GNR@PDA150). (C) DLS data of GNR@PDA150 showed a large size distribution (PDI ~ 0.2). (D) Optical extinction of GNR@PDA70 and GNR@PDA150. Longitudinal peak of GNR@PDA150 was not shown while GNR@PDA70 exhibited longitudinal peak around 1300 nm. This result indicated that longitudinal peak of GNR@PDA was no longer distinguishable when the PDA coating thickness became 150 nm.

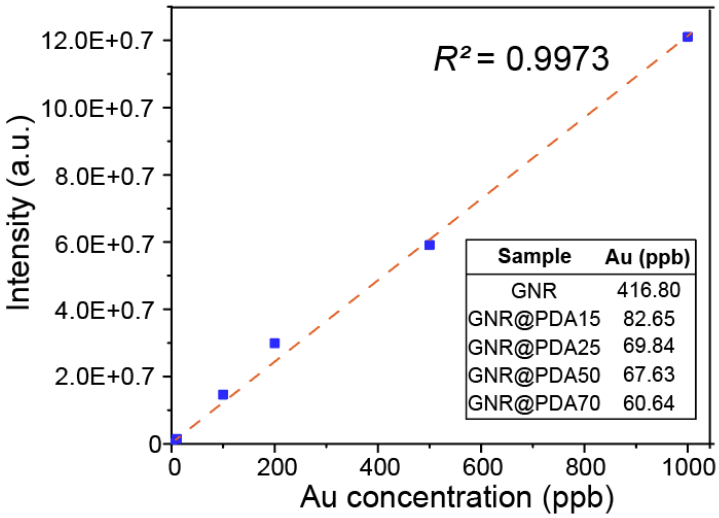

Figure S4. ICP-MS data. The number of GNRs in GNR, GNR@PDA15, GNR@PDA25, GNR@PDA50, and GNR@PDA70 was calculated by using ICP-MS method. Inset table indicates the concentration of Au ions in each sample solution.

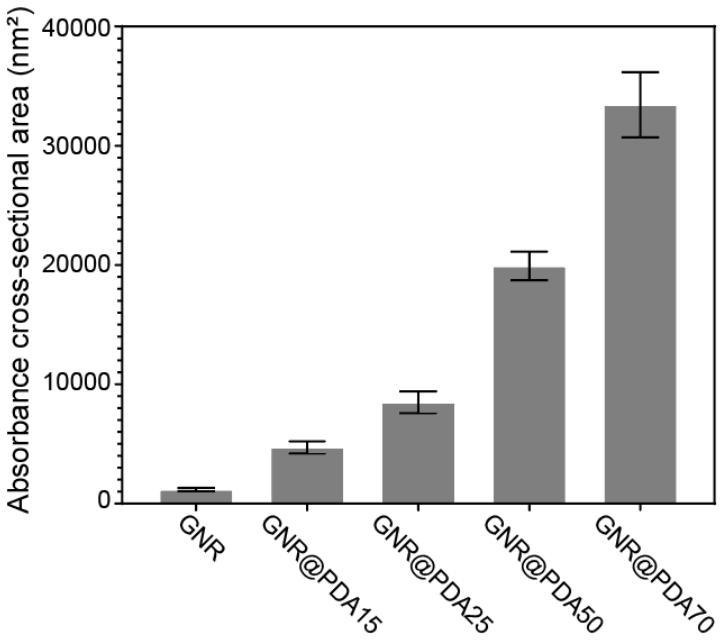

Figure S5. Absorption cross-sectional area of GNR@PDAs. Absorption cross-sectional area was exponentially increasing as PDA coating became thicker. Absorption cross-sectional area (nm^2) of GNR@PDA nanoparticles was calculated by the formula of diameter (D) × length (L) based on the TEM images. Error bar represents the standard deviation of fifteen GNR@PDA nanoparticles.

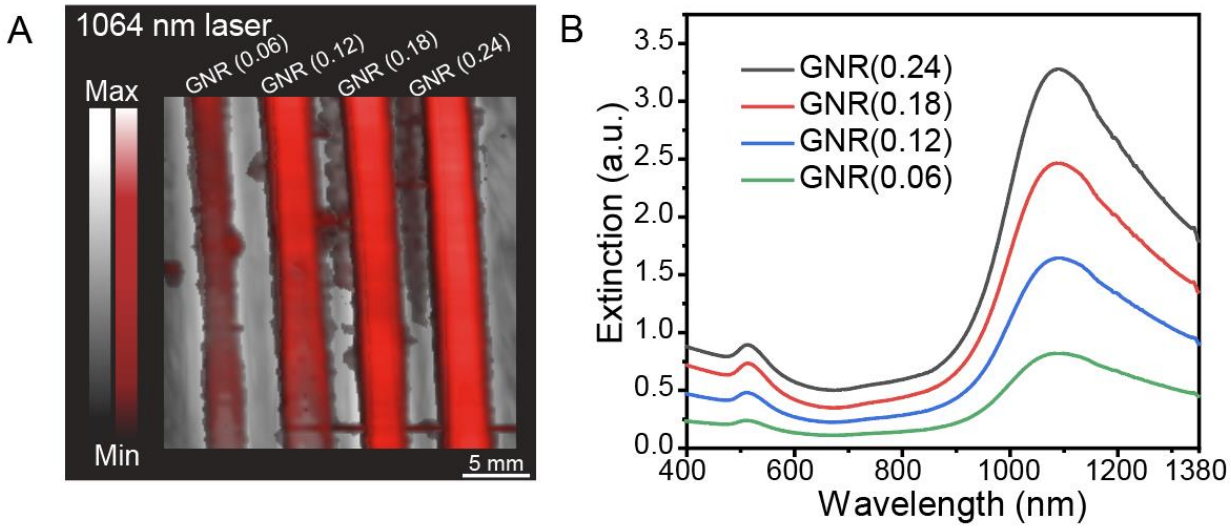

Figure S6. (A) PA image when illuminated with a 1064 nm laser, and (B) optical extinction of GNR at various concentrations (240, 180, 120, and 60 μg/mL). The optical absorption is proportional to the concentration leading to higher PA signal.

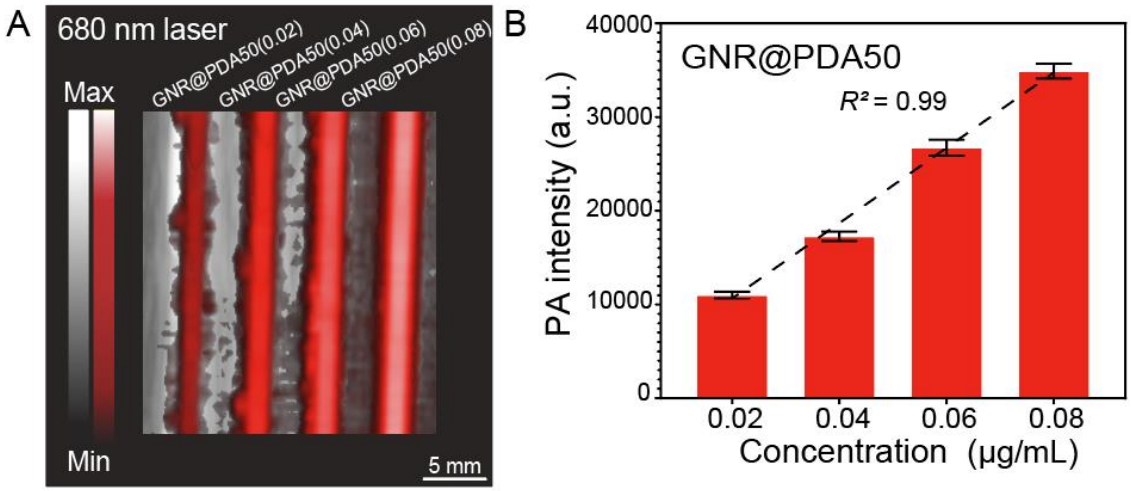

Figure S7. (A) PA image and (B) its corresponding quantitative PA signal amplitude of GNR@PDA50 when illuminated with a 680 nm laser. The increased concentration led to higher PA signal due to the increased absorbance. The error bar represents the standard deviation of five regions of interest.

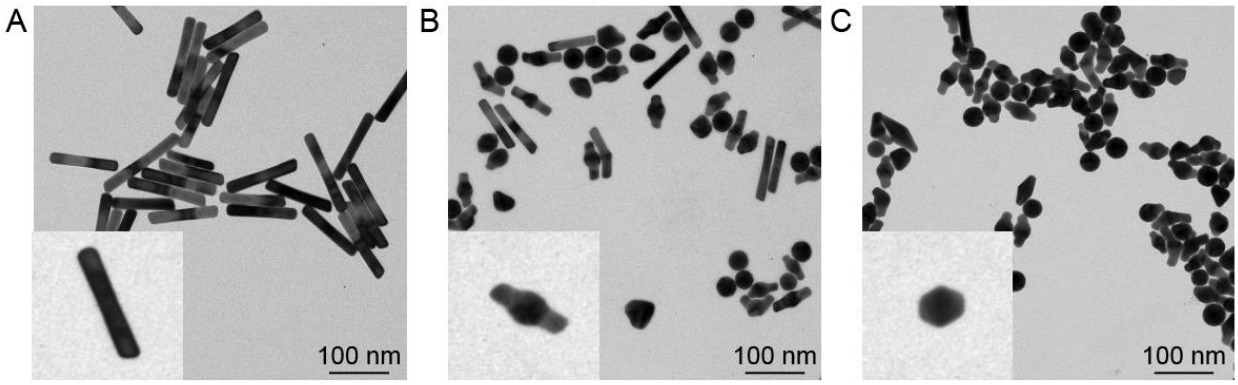

Figure S8. Shape transition of GNR under the laser illumination: (A) pristine GNRs, (B) shape transition of GNRs after 1 min of laser illumination, and (C) shape transition of GNRs after 5 min of laser illumination. Atomic rearrangement occurs at {110} facets of GNRs to minimize their surface energy, converting into spherical shape.

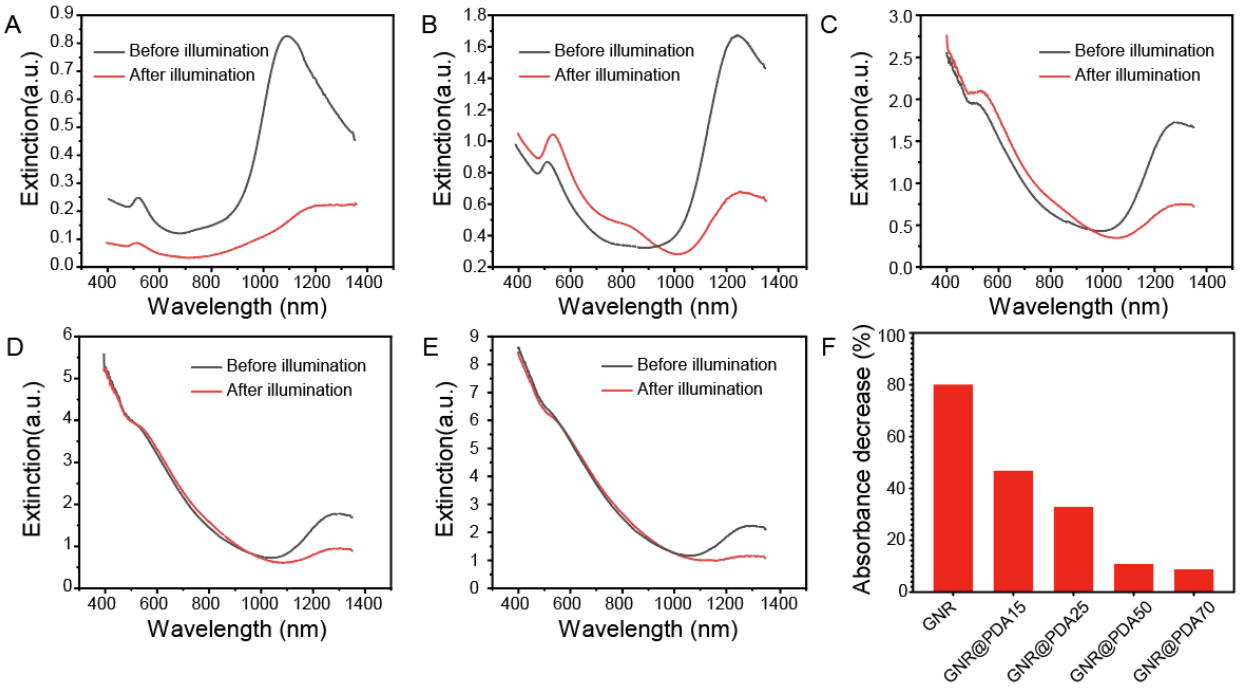

Figure S9. Changes of UV-vis-NIR spectra of GNR and GNR@PDAs before and after 5 min of the laser illumination. (A) GNR, (B) GNR@PDA15, (C) GNR@PDA25, (D) GNR@PDA50, (E) GNR@PDA70, and (F) longitudinal absorption peaks of GNR, GNR@PDA15, GNR@PDA25, GNR@PDA50, and GNR@PDA70 decreased by 80%, 47%, 33%, 11%, and 9%, respectively.

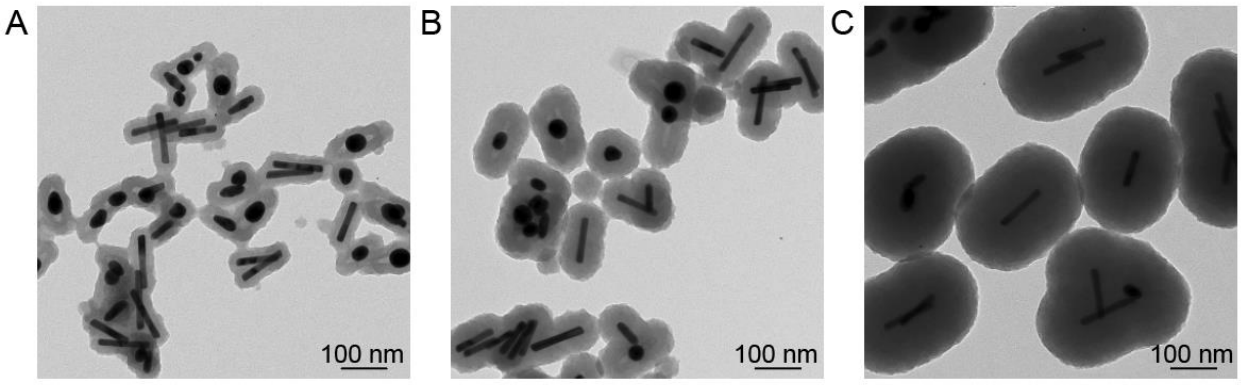

Figure S10. Shape transition of GNR@PDAs. (A) GNR@PDA15, (B) GNR@PDA25, and (C) GNR@PDA70 after 5 min of the laser illumination.

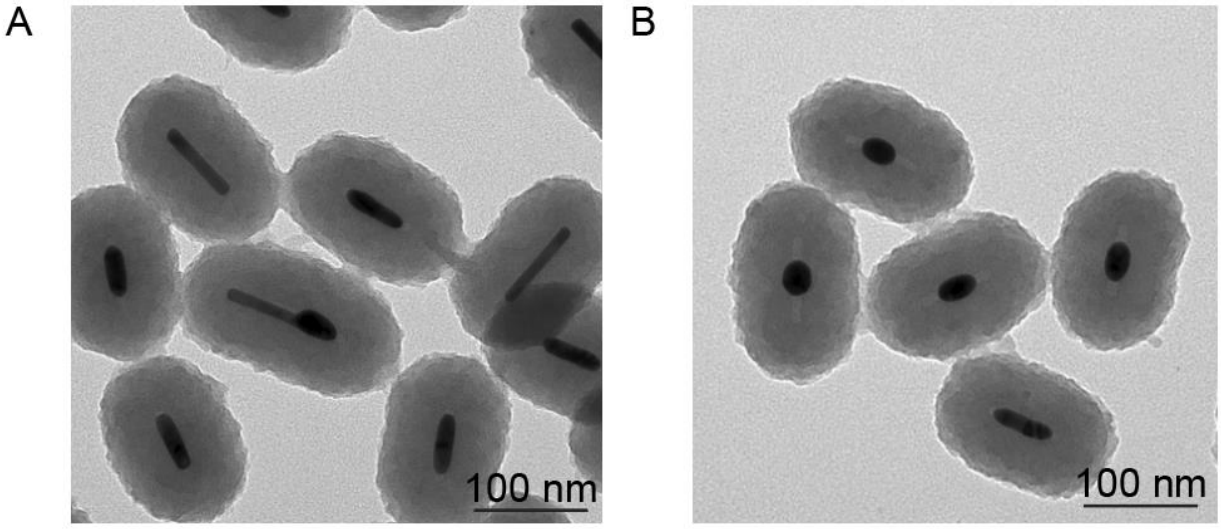

Figure S11. Shape transition of PDA@GNR50 after 5 min (A) and15 min (B) of the laser exposure. PDA coating maintained its original structure while most of the coated GNRs melt, showing that PDA is highly robust.

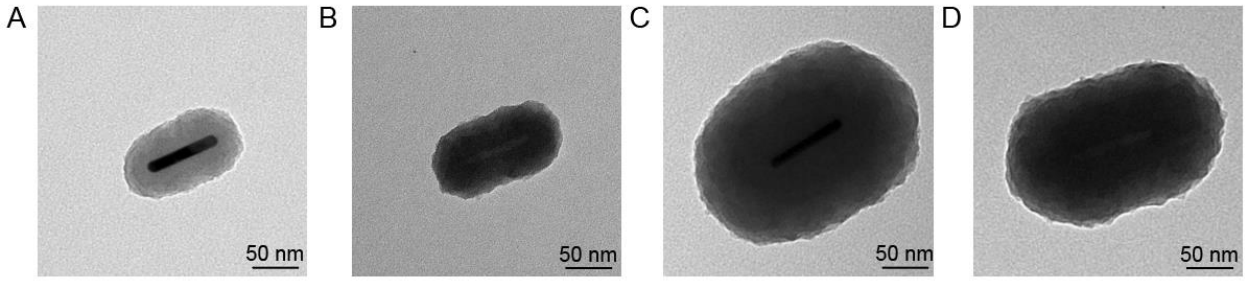

Figure S12. TEM images of single PDA capsule particle. (A) GNR@PDA15, (B) $PDA_{capsule}15$, (C) GNR@PDA70, and (D) $PDA_{capsule}70$.

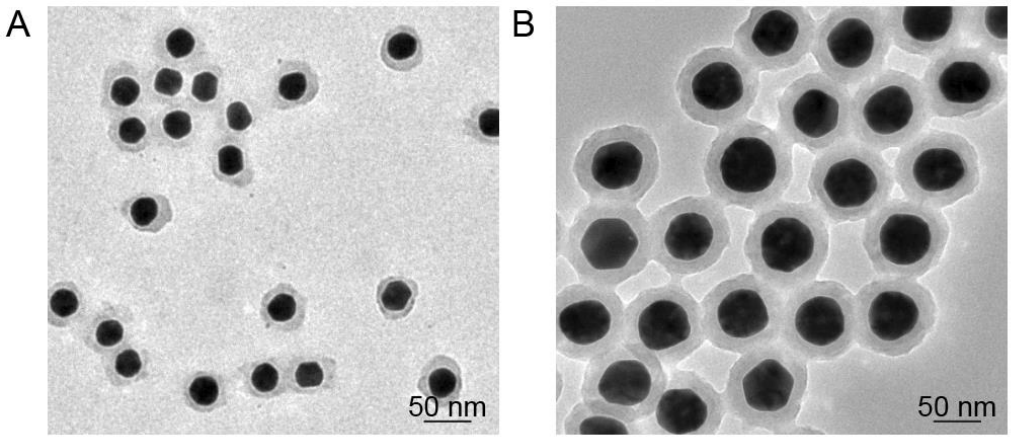

Figure S13. PDA coated gold nanospheres (GNSs): (A) 30 nm and (B) 60 nm GNSs covered by PDA shell. These images indicate that PDA coating strategy can be applied to various types of nanoparticles for improving PA performance.

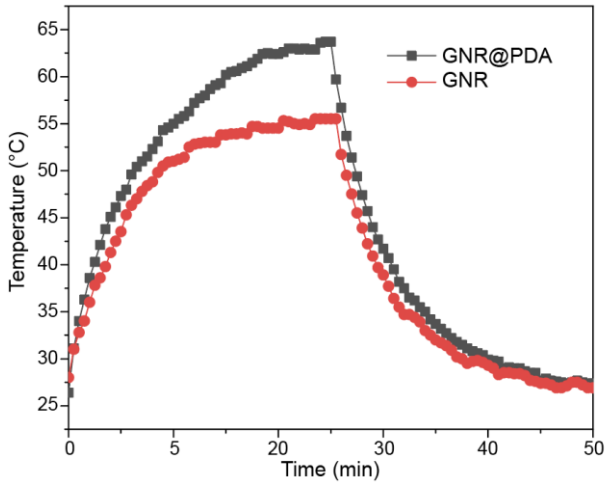

Figure S14. Photothermal conversion efficiency of GNR and GNR@PDA. Photothermal conversion efficiency of GNR@PDA (40 %) was 2 % higher than that of GNR (38 %), indicating that PDA coating can be used for photothermal therapy. 1064 nm laser with 1 W/cm^2 was used for the measurement.

Calculation of mushroom and brush conformation of PEG chain.

Based on the Flory – Huggins theory, brush conformation will be formed when the graft density is high (D > F). Thus, we need to calculate Flory radius (F) by using below equation (1).[1]

$F = n^{3/5}\alpha$ (1)

where n is the number of monomers per chain, and a is a monomer size (α =3.5Å for PEG).[2] After calculating F, we can estimate the minimum D to have brush conformation (D > F). For example, $F = 120^{3/5}*3.5^2$ (n is about 120 when a molecular weight of PEG is 5000). Thus, D > F ≈ 216.6 Å is required to make brush conformation.

Next, the surface area of single gold nanorod (GNR) nanoparticle can be calibrated by following equation (with an assumption that GNR has a perfect cylindrical shape.)

$A = \pi r^2+4rL$ (2)

where A is surface area of GNR, r is half diameter of GNR, and L is length of GNR. Then, we can divide the surface area of a single GNR nanoparticle with D^2 to know the minimum number of PEG-chains to cover a single GNR nanoparticle. For example, r and L of GNR were 6.23 ± 0.68, and 95.07 ± 6.92 nm respectively (see **Table 1**). Surface area of a single GNR nanoparticle was about 2489.33 nm^2, and D^2 is 470.89 nm^2. Thus, minimum number of PEG-SH molecule was about 20 to cover a single GNR nanoparticle under the premise that all the PEG-SH molecule is substituted with CTAB. With this information, we can estimate the minimum amount of PEG-SH solution to make brush conformation when we know the concentration of GNR by ICP-MS method (**Figure S5**).

Detailed information about Equation 5

Shape transition of GNRs can be also explained by absorbance decrease according to equation 1.[3]

$[(A_{\lambda,0} - A_{\lambda,1})/\sigma b)] = \rho\sigma^{(n)}I^{(n)}$ (1)

where $A_{\lambda,0}$ is the sample absorbance at a given wavelength (λ) before the laser illumination, $A_{\lambda,1}$ is the sample absorbance at a given wavelength (λ) after the laser illumination, σ is the absorption cross-section of the nanoparticles, b is the path length, ρ is the density of the nanoparticles, and n is the number of photons absorbed. I is laser fluence.

$[(A_{\lambda,0} - A_{\lambda,1}/b)] = \rho\sigma^{(n)+1}I^{(n)}$ ---- multiply σ

$[(A_{\lambda,0} - A_{\lambda,1}/c\varepsilon b)] = (\rho\sigma^{(n)+1}I^{(n)})/c\varepsilon$ ---- (2)

c: concentration, ε: molar extinction coefficient

Applying the Beer-Lambert Law ($A_{\lambda,0}$= cεb) to equation (2)

$(A_{\lambda,0} - A_{\lambda,1})/A_{\lambda,0} = (\rho\sigma^{(n)+1}I^{(n)})/c\varepsilon$ ---- (3)

ln $[(A_{\lambda,0} - A_{\lambda,1})/A_{\lambda,0}]$ = ln $(\rho\sigma^{(n)+1}I^{(n)})/c\varepsilon$ ---- applying ln to both sides of equation (3)

ln $[(A_{\lambda,0} - A_{\lambda,1})/A_{\lambda,0}]$ = ln $I^{(n)}/c\varepsilon$ + ln $(\rho\sigma^{(n)+1})$/cε ---- cε << $I^{(n)}$

Equation (1) can be rearranged to

$ln\ [(A_{\lambda,0} - A_{\lambda,1})/A_{\lambda,0}]$ = nln(I) + constant

References

(1) de Gennes, P. Conformations of Polymers Attached to an Interface. *Macromolecules* **1980,** *13* (5), 1069-1075.
(2) Jokerst, J. V.; Lobovkina, T.; Zare, R. N.; Gambhir, S. S. Nanoparticle PEGylation for Imaging and Therapy. *Nanomedicine* **2011,** *6* (4), 715-728.
(3) Gandhi, S. R.; Bernstein, R. B. Influence of the Focal Length of the Laser Beam Focusing le ns on MPI yield. *Chem. Phys.* **1986,** *105* (3), 423-434.